

Article

Comparative Transcriptome Analysis and Expression of Genes Associated with Polysaccharide Biosynthesis in *Dendrobium officinale* Diploid and Tetraploid Plants

Phu Long Pham¹, Thi Tuyet Cham Le¹, Thi Thuy Hang Vu¹, Thanh Tuan Nguyen¹, Zhi-Sheng Zhang², Rui-Zhen Zeng², Li Xie², Minh Ngoc Nguyen³, Vuong Thi Huyen Trang³, Tran Dang Xuan^{4,*} 
and Tran Dang Khanh^{3,*} 

¹ Faculty of Agronomy, Vietnam National University of Agriculture, Hanoi City 131000, Vietnam; lttcham@vnua.edu.vn (T.T.C.L.)

² College of Forestry and Landscape Architecture, South China Agricultural University, Guangzhou 510642, China

³ Department Genetic Engineering, Agricultural Genetics Institute, Pham Van Dong Street, Hanoi City 122000, Vietnam; vuongthihuyentrang@gmail.com (V.T.H.T.)

⁴ Department of Development Technology, Graduate School for International Development and Cooperation, Hiroshima University, Hiroshima 739-8529, Japan

* Correspondence: tdxuan@hiroshima-u.ac.jp (T.D.X.); tdkhanh@vaas.vn (T.D.K.); Tel.: +84-9164-51018 (T.D.K.)

Abstract: *Dendrobium officinale* Kimura et Migo is a kind of herb with high medicinal, ornamental, and commercial value, and is rich in polysaccharides. Polyploid breeding is an important breeding method for the genome doubling of medicinal species to increase biomass and polysaccharide production. Previous studies have revealed comparative transcriptome analysis and polysaccharide biosynthesis across the growth stages and plant parts, but there have been no studies dissecting such genes and pathways in tetraploid *D. officinale*. Therefore, this study aimed to unravel the molecular mechanisms of the increase in polysaccharide content in tetraploid *D. officinale* via the generation of four transcriptomic libraries for protocorm-like bodies and six-month-old seedlings of both diploid and tetraploid *D. officinale* plants. In this study, a total of 230,786,618 clean reads remained with a total of 34.62 Gb nucleotides generated; 274,403 unigenes were assembled, of which 73.99% were annotated to at least one of the protein databases; and of 17,451 unigenes, 6.35% were annotated to all seven protein databases (NR, NT, KO, Swiss-Prot, FAM, GO, and KOG). Putative genes encoding enzymes related to polysaccharide biosynthetic pathways were determined. RT-qPCR for 11 randomly selected genes involved in polysaccharides indicated consistency with RNA-Seq data and polysaccharide content. The expressions of nine genes were higher in tetraploid than in diploid plants, while the expressions of the other two genes encoding bifunctional enzymes were the opposite. This study has provided a foundation for subsequent works regarding the biosynthetic pathways of metabolites involved in the autopolyploidy of *Dendrobium* species in general, and *D. officinale* in particular.

Keywords: *Dendrobium officinale*; polysaccharides biosynthesis; pathway; transcriptome



Citation: Pham, P.L.; Le, T.T.C.; Vu, T.T.H.; Nguyen, T.T.; Zhang, Z.-S.; Zeng, R.-Z.; Xie, L.; Nguyen, M.N.; Trang, V.T.H.; Xuan, T.D.; et al. Comparative Transcriptome Analysis and Expression of Genes Associated with Polysaccharide Biosynthesis in *Dendrobium officinale* Diploid and Tetraploid Plants. *Agronomy* **2024**, *14*, 69. <https://doi.org/10.3390/agronomy14010069>

Academic Editor: Radoslaw Suchecki

Received: 12 September 2023

Revised: 13 December 2023

Accepted: 21 December 2023

Published: 27 December 2023



Copyright: © 2023 by the authors. Licensee MDPI, Basel, Switzerland. This article is an open access article distributed under the terms and conditions of the Creative Commons Attribution (CC BY) license (<https://creativecommons.org/licenses/by/4.0/>).

1. Introduction

Polysaccharides are essential biological macromolecules that have recently been demonstrated to have potential biological effects, especially in the field of pharmaceutical medicine [1,2]. They demonstrate a broad spectrum of biological and pharmacological functions, such as anti-oxidant, anti-diabetic, anti-tumor, anti-microbial, anti-coagulant, anti-viral, immunomodulatory, and hypoglycemic activities [1,3–5]. Various types of polysaccharides, including arabinogalactans, pectic polysaccharides, glucans, mannans, galactans, fucoidans, fructans, hyaluronans, and xylans, have been extracted from different sources like marine algae, mushrooms, bacteria, and especially from herbal plants [6–8].

However, polysaccharides with diversified structures from different origins exhibit a variety of biological activities [8].

The genus *Dendrobium* is one of the largest genera in the family Orchidaceae, including approximately 1200–1500 species, and is mainly found in subtropical and tropical areas in Asia and eastern Australia [9]. In China alone, there are around 120 species, and half of them have been reported to possess medicinal properties [10,11]. The basic chromosome number of most *Dendrobium* is $2n = 2x = 38$, a few are $2n = 2x = 40$, and a small number are $2n = 2x = 36$ [12,13]. The *D. officinale* plant species ($2n = 2x = 38$) is a highly evolved and specialized endangered species within the *Dendrobium* genus. Recent efforts of worldwide scientists in *D. officinale* breeding, including germplasm collection, identification, evaluation, and conventional hybridization, have been made. However, most breeding programs have mainly focused on enhancing morphological traits and biomass production [14].

Chromosome manipulation is a feasible way to improve the quality traits of *Dendrobium* species and various ornamental crops [15,16]. Through colchicine treatment, autopolyploids have been induced in various *Dendrobium* species, namely, *D. chrysotoxum* [17], *D. devonianum* [18], *D. nobile* [19], *D. ochreatum* [20], and *D. officinale* [21,22]. Presently, approximately 20 registered hybrids have emerged from both intra- and inter-sectional hybridization of *D. officinale*. However, a sporadic number of cultivars have been released based on tetraploid germplasm for cross-breeding programs [13].

D. officinale is currently an important herb appreciated for its ornamental value and medicinal properties. It has been reported to have a broad range of therapeutic effects in many countries in Asia [8,23,24]. This plant species is rich in polysaccharides, which also depend on the growth stages and plant parts [25–27]. To the best of our knowledge, over 190 constituents have been isolated from *D. officinale*, including polysaccharides, alkaloids, bilphenanthrene, bibenzyl, flavonoids, essential oil, amino acids, and several trace mineral elements [28,29]. These polysaccharides consist mainly of glucose and mannose, as well as trace amounts of arabinose, xylose, and galactose. *D. officinale* stems have been demonstrated to have the highest content of polysaccharides and the best medical properties [27,30]. Consequently, demand for this herb is growing, which causes over-harvesting from nature. This, coupled with difficult growing conditions, leads to an increasing demand for propagation, domestication, and breeding of this herb to increase productivity.

Polyploidization is a useful breeding tool for increasing biomass/yield, and has been used as a strategy to alter the quantitative and qualitative patterns of secondary metabolite production in various medicinal plants [31]. Its general effects on change in the phenotypic, biochemical, and genetic traits are well described in some medicinal plant species. For example, polyploidization has been successfully applied to increase the size of organs like the leaves and stomata of *Stevia rebaudiana* [32] and *Artemisia annua* L. [33,34]; the roots and stems of *S. miltiorrhiza* Bge [35] and *Scutellaria baicalensis* [36]; and the biomass of *Panax ginseng* [37] and *Cymbopogon* spp. [38]. Our previous study indicated that tetraploid *D. officinale* has shorter leaves as well as shorter and thicker stems and roots, and produces more biomass than its diploid progenitors [39]. Polysaccharide contents in the stems, leaves, and roots of 6-month-old tetraploid plantlets were significantly higher than those diploids. Moreover, the polysaccharide contents in the stems of tetraploid *D. officinale* “201-1-T” were increased by about twofold compared with the diploid plants [39]. Polysaccharides are one of the main bioactive constituents, and these contents determine the quality of *D. officinale*. So far, some transcriptomes of *D. officinale* have been sequenced to identify genes involved in polysaccharide biosynthesis. He et al. [40] suggested that the *CELLULOSE SYNTHASE LIKE A* family gene (*CSLA*) is involved in the biosynthesis of bioactive mannan polysaccharides. Zhang et al. [41] also identified the genes related to polysaccharide biosynthesis, which included 430 glycosyltransferase genes (GTs) and 89 cellulose synthase genes (CesA). Moreover, three GT genes, one frucosyltransferase gene, and one mannosyltransferase gene showed specific expression in *D. officinale* stems [42]. Most studies have revealed transcriptomic profiles and polysaccharide biosynthesis using diploid *D. officinale* at different growth stages from juvenile to adult [41] or different plant parts (stem, leaves, and

roots) [43], protocorm-like bodies, and leaves [26,27]. However, the genes involved in the biosynthesis of polysaccharides in tetraploid *D. officinale* currently remain unknown. Therefore, our study aimed to investigate the molecular mechanisms underlying polysaccharide content in tetraploid *D. officinale* using RNA-Seq data of protocorm-like bodies (PLBs) and six-month-old seedlings to compare and identify the genes involved in polysaccharide biosynthesis in PLBs and the seedlings of diploid and tetraploid *D. officinale*.

2. Materials and Methods

2.1. Plant Materials and Growth Conditions

An elite diploid line ($2n = 38$) selected from hybrid combinations of *D. officinale* “Beijingsanyi” \times *D. officinale* “Husonghua” (denoted as 201) and its respective tetraploid ($2n = 76$) was used in this study. Tetraploid was generated as previously described by Pham et al. [39]. In short, the diploid hybrid 201-1 was induced by colchicine. The tissue callus of 201-1 was cultured in agar-free MS media with the addition of 1 ppm colchicine. The culture was then shaken circularly at 120 rpm (25 °C) for 3 days. Subsequently, the callus was removed and washed three times with distilled water, then transplanted into MS medium supplemented with 0.2 ppm of BA and 0.1 ppm of NAA, respectively. After 2 months of in vitro cultivation, the tetraploid plants were examined by chromosome analysis and flow cytometry [39].

For transcriptome analysis, diploid hybrid 201-1 (denoted as A) and autotetraploid 201-1-T (denoted as B) of *D. officinale* at two development stages (protocorms-like bodies and 6-month-old seedlings) were used. Different concentrations of 6BA, NAA, and AC were used appropriately for cultures at different growth stages (Table S1). For transcriptomic analysis, 80 protocorms-like bodies (PLBs) and 15 seedlings of six-month-old seedlings for each diploid A and tetraploid B were yielded, frozen rapidly in liquid nitrogen, and kept at -80 °C for later RNA extraction. For qRT-PCR validation and gene expression profiling analysis, stems of six-month-old seedlings were used. Seedlings were grown in small pots in tissue culture room conditions (25 ± 1 °C), with a light/dark cycle of 16/8 h and 66–70% relative humidity.

2.2. RNA Isolation, cDNA Library Preparation, Transcriptome Sequencing

Total RNA was isolated from 100 mg of plant material utilizing the OmniPlant RNA Kit (Cwbio, Beijing, China). The OD_{260/280} was scrutinized within the range from 1.8 to 2.1 to ensure the purity of the RNA samples. RNA integrity was applied by agarose gel electrophoresis (1.0%) using an Agilent 2100 Bio-analyzer (Agilent Technologies, Santa Clara, CA, USA) with RIN number > 7.5 . Each sample was then subjected to an input of 3 μ g of RNA. According to the manufacturer’s guidelines, the transcriptome analysis samples were prepared using the TruSeq™ RNA Sample Preparation Kit from Illumina, San Diego, CA, USA. Initially, mRNA was extracted from the total RNA using magnetic beads coated with oligo (dT), and these mRNA molecules were subsequently fragmented by adding a fragmentation buffer. Next, we performed a synthesis of first-strand cDNA using random hexamer primers (short fragments as templates), which were then used to synthesize the second-strand cDNA. The products were purified and enriched by PCR to generate the final cDNA libraries. The prepared libraries were subjected to sequencing on an Illumina HiSeq 2500 platform, yielding 125 base pair paired-end reads.

2.3. De Novo Assembly and Functional Annotation

In order to attain clean reads, we removed the low-quality reads and adapter sequences using SeqPrep (<https://github.com/jstjohn/SeqPrep>, accessed on 12 September 2023) and Sickle (<https://github.com/najoshi/sickle>, accessed on 12 September 2023). All clean reads were then assembled using the Trinity software tool [44] based on the left.fq and right.fq, with the min_kmer_cov set to 2 and all other parameters set as their defaults. To perform function annotation, the longest transcript of each gene was defined as the “unigene”. Subsequently, nucleotide sequences of all unigenes were searched against the current versions

of NR (NCBI non-redundant protein sequences) [45]; NT (NCBI nucleotide sequences); GO (gene ontology), with a reference at (<http://www.geneontology.org>, accessed on 12 September 2023) [46]; KEGG (Kyoto Encyclopedia of Genes and Genomes) databases [47]; KOG (eukaryotic orthologous groups of proteins); Swiss-Prot (a manually annotated and reviewed protein sequence database), with a reference at (<http://www.ebi.ac.uk/uniprot>, accessed on 12 September 2023) [48]; PFAM 32.0 (protein family), with a reference at (<http://pfam.sanger.ac.uk/>, accessed on 12 September 2023) [49]; and String 10.0 (search tool for the retrieval of interacting genes) [50], applying BLAST2GO version 2.5 with a cut-off E-value of 10^{-5} [51]. To identify genes involved in carbohydrate activity, all unigenes were examined against the CAZy database using BLAST 2.7.1 with a cut-off e-value of 10^{-5} .

2.4. Identification of Differentially Expressed Genes (DEGs)

Gene expression levels were estimated by mapping clean reads to the Trinity transcript assembly using RSEM version 1.2.15 [52], with the bowtie2 parameter set at mismatch 0. Differential expression analysis was applied by edgeR [53]. The thresholds for significant differential expression were a false discovery rate (FDR) of <0.05 and a $[\log_{10}(\text{fold change})] \geq 1$. The identified DEGs were applied for GO and KEGG enrichment analyses.

2.5. Quantitative Real-Time PCR (qRT-PCR) Validation

qRT-PCR for gene expression profiling analysis was conducted using RNA samples extracted from the stems of six-month-old seedlings of diploid 201-1 and tetraploid 201-1-T, with three biological replicates. Eleven unigenes associated with polysaccharide molecular function were randomly selected for qRT-PCR, including *DoCSLA3-1*, *Dog1gC1*, *Dog1gC3-1*, *DoGMPP-1*, *DoGMPP-2*, *DoGMPP-3*, *Dogmpl*, *DoMAN2-2*, *DoPGM1*, *DoPGM2-2*, and *DoPMM2-1*. Primers were designed using StepOne Software 2.3 (Table S2).

Total RNA was extracted from the stems of six-month-old seedlings using an Omni-Plant RNA Kit, then checked for purity and integrity as described above. Total RNA was reverse-transcribed to synthesize the first-strand cDNA (first strand cDNA Synthesis Kit, TaKaRa) according to the manufacturer's protocol. The qRT-PCR was performed on an ABI 7500 Real-time PCR system (Applied Biosystems, Foster City, CA, USA) using SYBR Premix Ex Taq (Takara Bio Inc., Shiga, Japan) according to the manufacturer's protocol.

Expression levels were normalized against *Actin* and calculated by the ($2^{-\Delta\Delta C_t}$) method [54]. Glyceraldehyde 3-phosphate dehydrogenase (GAPDH) was used as a reference gene for each sample. Real-time PCR was performed with three replicates for each sample, and data are given as mean \pm SD ($n = 3$). Pearson correlation analysis was used to determine the consistency of the RNA-seq and qRT-PCR data.

3. Results

3.1. Transcriptome Sequencing and De Novo Assembly

In order to determine the *D. officinale* transcriptome expression profile, next-generation sequencing was conducted on diploid and tetraploid *D. officinale* 201-1 (A) and 201-1-T (B) at two different growth stages: protocorm-like bodies (P) and six-month-old seedlings (D), respectively. Four cDNA libraries were constructed, including protocorm-like bodies of diploid plants (AP), protocorm-like bodies of tetraploid plants (BP), seedlings of diploid plants (AD), and seedlings of tetraploid plants (BD). In total, 235,443,082 raw reads were generated (Table 1), including raw reads of AP (56,991,166), BP (55,980,546), AD (60,575,150), and BD (61,896,220), respectively. After removing adaptor sequences, ambiguous nucleotides, and low-quality sequences, 230,786,618 clean reads remained, with a total of 34.62 Gb nucleotides. The base average error rates were 0.02 to 0.03%; the average Q20 and Q30 values were 98.01 and 94.26%, respectively; and the average GC content was 46.44% (Table 1).

Table 1. Summary of Illumina transcriptome sequencing of PLBs and 1-, 2-, and 6-month-old seedlings of diploid and tetraploid *D. officinale*.

Samples	Raw Reads	Clean Reads	Clean Bases (Gb)	Error/%	Q20/%	Q30/%	GC/%
AP	56,991,166	55,610,478	8.34	0.02	98.07	94.4	45.98
BP	55,980,546	55,178,130	8.28	0.03	98.01	94.24	46.50
AD	60,575,150	59,332,712	8.90	0.02	98.04	94.31	46.45
BD	61,896,220	60,665,298	9.10	0.03	97.93	94.10	46.82
Total Average	235,443,082	230,786,618	34.62		98.01	94.26	46.44

AP—protocorm-like bodies of diploid plants; BP—protocorm-like bodies of tetraploid plants; AD—seedlings of diploid plants; BD—seedlings of tetraploid plants; Q20—percentage of bases with a Phred value > 20; Q30—percentage of bases with a Phred value > 30; error (%)—base error rate; GC (%)—percentage of bases with G and C numbers in the total number of bases.

All clean reads were assembled to generate unigenes. The assembly of the clean reads produced 274,403 unigenes and 416,641 transcripts, with the highest 84,270 unigenes and 90,037 transcripts ranging from 501–1000 bp in length (Table 2).

Table 2. Splicing length frequency distribution.

Transcript Length Interval	200–500 bp	500 bp–1 kbp	1–2 kbp	>2 kbp	Total
Number of transcripts	235,579	90,037	63,469	27,556	416,641
Number of unigenes	99,607	84,270	62,998	27,528	274,403

3.2. Functional Annotation of *D. officinale* Transcriptome

A total of 274,403 unigenes were annotated using multiple public databases, and the number and percentage of unigenes matched seven protein databases (Table 3; Figure 1). In summary, 131,990 unigenes (48.10%), 183,742 unigenes (66.96%), 45,601 unigenes (16.61%), 90,095 unigenes (32.83%), 89,223 unigenes (32.51%), 89,827 unigenes (32.73%), and 29,056 unigenes (10.58%) were annotated to NR, NT, KO, Swiss-Prot, FAM, GO, and KOG, respectively. A total of 203,043 unigenes (73.99%) were annotated to at least one of the protein databases, while 17,451 unigenes (6.35%) were annotated to all seven protein databases.

Table 3. Summary of unigene annotations to seven databases.

Component	Number of Unigenes	Percentage (%)
Annotated in NR	131,990	48.10
Annotated in NT	183,742	66.96
Annotated in KEGG	45,601	16.61
Annotated in Swiss-Prot	90,095	32.83
Annotated in PFAM	89,223	32.51
Annotated in GO	89,827	32.73
Annotated in KOG	29,056	10.58
Annotated in all databases	17,451	6.35
Annotated in at least one database	203,043	73.99
Total unigenes	274,403	

NR = NCBI non-redundant protein sequences, NT = NCBI nucleotide sequences, KEGG = Kyoto encyclopedia of genes and genomes; PFAM = protein family, GO = gene ontology; KOG = eukaryotic orthologous groups of proteins.

The E-value distribution of the top hits in our NR database analysis demonstrated that 50% of the top hits showed high homology, with an E-value < 1.01×10^{-50} (Figure 2). The similarity distribution indicated that 80.88% of the unigenes showed a similarity higher than 60%, and 19.40% of unigenes had a similarity between 40–60% (Figure 2b). Based on NR annotation, the unigenes with the best scores were assigned to sequences from the top

five species: *Elaeis guineensis* (27.7%), *Phoenix dactylifera* (24.5%), *Nelumbo nucifera* (3.2%), *Musa acuminata* (10.4%), and *Vitis vinifera* (3.8%). The remaining 30.4% of the contigs were unknown (Figure 2c).

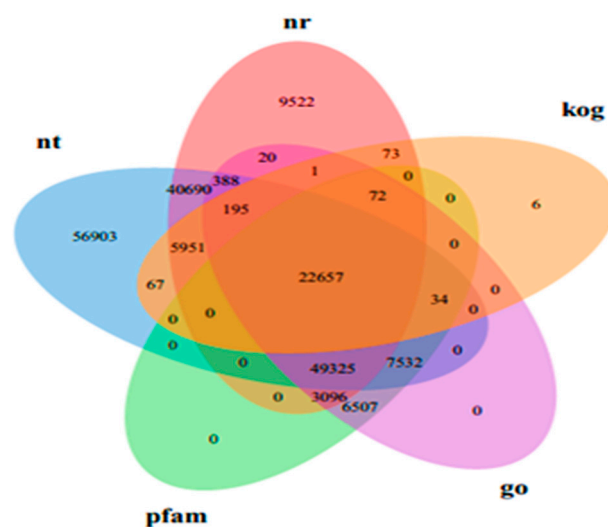


Figure 1. BLAST results for *D. officinale* transcripts. The Venn diagram demonstrates the distribution of annotated contigs against five public protein databases, including NR, NT, KOG, GO, and PFAM.

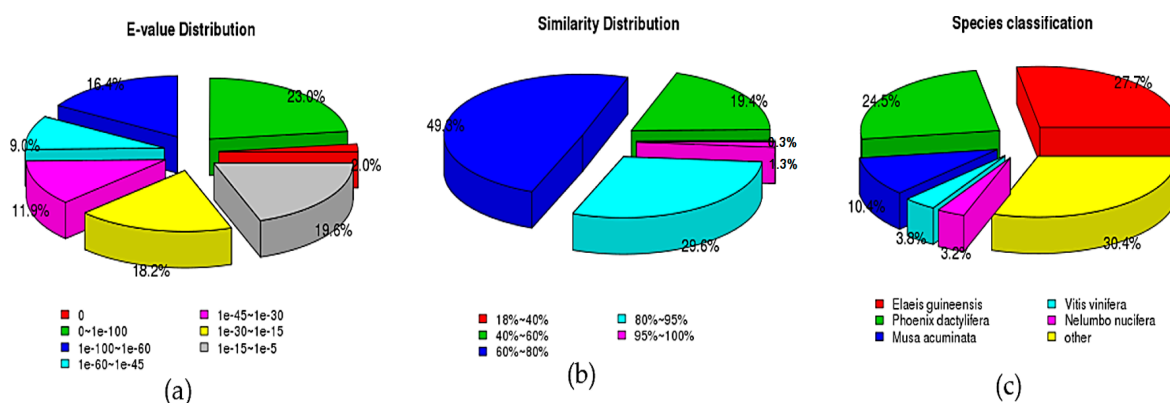


Figure 2. Characteristics of sequence homology of *D. officinale* hybrids BLASTED against the NCBI non-redundant (NR) database. (a) e-value distribution of BLAST hits for matched unigene sequences using an e-value cutoff of 1.0×10^{-5} ; (b) similarity distribution of top BLAST hits for each unigene; (c) species distribution of the top BLAST hits.

Through GO classification, 89,827 unigenes were grouped into 57 functional groups. Among them, 26 groups were related to biological processes, 21 groups were involved in cellular components, and 10 groups were involved in molecular function (Figure 3). In the biological process category, metabolic processes and cellular processes were mostly dominant. Within the molecular function category, a high percentage of the genes were involved in binding and catalytic activity. Most assignments in cellular components were made to cell components and cell membranes.

Through KOG classification, a total of 29,057 unigenes were classified into 25 subgroups (Figure 4). Among these, R (general function prediction only) was the top subgroup, followed by O (post-translational modification, protein turnover, and chaperones) and J (translation, ribosomal structure, and biogenesis). In this study, a total of 34,394 sequences were assigned to 19 KEGG pathways, of the top five pathways were metabolism (A, 2108 unigenes), genetic information processing (B, 1564 unigenes), environmental information processing (C, 8680 unigenes), cellular process (D, 20,583 unigenes), and organismal systems (E, 1549 unigenes) (Figure S1). The top three subcategories of pathways were

carbohydrate metabolism (3986 unigenes, 11.59%); translate (3317 unigenes, 9.64%); and folding, sorting, and degradation (2873 unigenes, 8.35%). These annotations have provided a valuable resource for examining the specific functions, pathways, and processes involved in polysaccharide biosynthesis and *D. officinale* development.

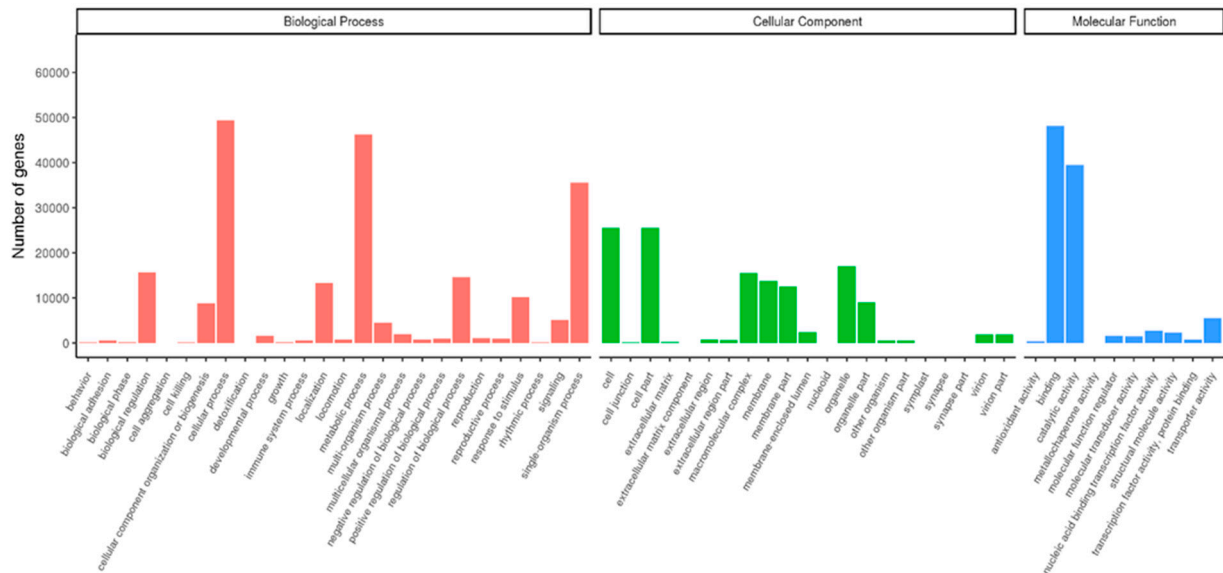


Figure 3. Gene ontology categories of *D. officinale* unigenes with biological processes, cellular components, and molecular function.

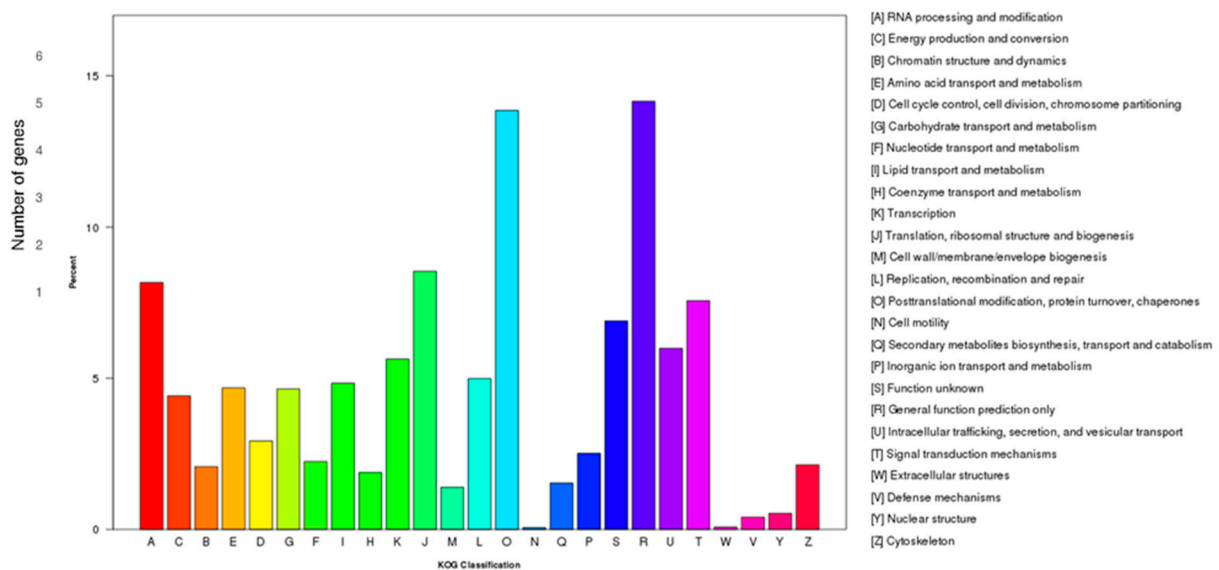


Figure 4. KOG functional classification of *D. officinale* unigenes. A total of 29,057 unigenes were classified into 25 functional categories following their predicted gene products using the KOG database (cut-off E-value of 0.00001). The x-axis presents the names of 25 groups of KOG; the y-axis indicates the percentage of unigenes.

In addition, different kinds of glycosyltransferases genes (GTs) were identified, with 127, 94, 26, and 29 genes for glucosyltransferases, mannosyltransferases, fucosyltransferases, and xylosyltransferases, respectively (Table S2). In the KEGG pathway, genes involved in carbohydrate metabolism, such as fructose and mannose metabolism (ko00051) and galactose metabolism (ko00052), were identified (Table S2).

3.3. Screening and Identification of DEGs

Differentially expressed genes (DEG) were identified between the genotypes of *D. officinale* (201-1 and 201-1-T) at the stages of protocorm-like bodies (PLBs) and six-month-old seedlings (Figures 5–7). Unigenes with Q-values < 0.005 and $|\log_2FC| > 1$ were defined as DEGs between organs/genotypes. When $\log_2FC > 1$, DEG was judged to be up-regulated, while $\log_2FC < -1$, was scrutinized as a downward adjustment.

Based on the transcriptome data, all DEGs were applied for hierarchical cluster analysis of transcription abundance in the different growth stages. The heatmap of DEGs between different growth stages of diploid A and tetraploid B shows similar transcriptome profiles for AP, AD, BP, and BD (Figure 5).

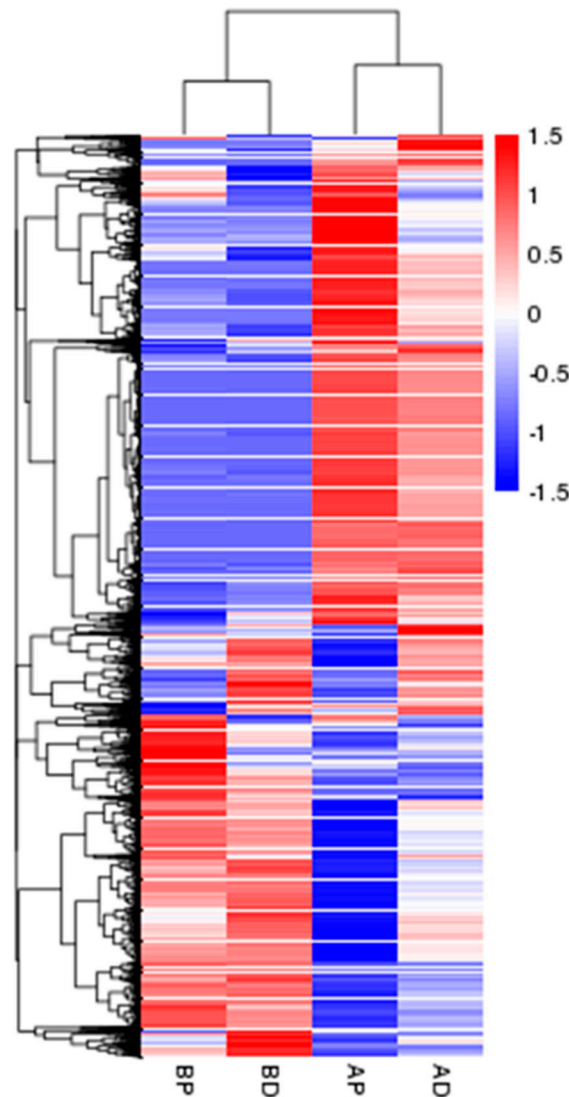


Figure 5. Heat map illustrating the expression profiles of diploid (A) and tetraploid (B) *D. officinale* hybrids (201-1 and 201-1-T, respectively) at the stages of protocorm-like bodies (P) and seedlings (D). Each column represents a sample, and each row implies a gene. The colors in the graph show the magnitude of gene expression in the sample. Red implies that the gene was highly expressed in the sample, and blue indicates that the gene expression was low. AP—protocorm-like bodies of diploid plants; BP—protocorm-like bodies of tetraploid plants; AD—six-month-old seedlings of diploid plants; BD—six-month-old seedlings of tetraploid plants.



Figure 6. Venn diagram of the unigenes for diploid (A) and tetraploid (B) *D. officinale* hybrid plants (201-1 and 201-1-T, respectively) at the stages of protocorm-like bodies (P) and six-month-old seedlings (D). The diagram shows the overlapping unigenes (a) between protocorm-like bodies of diploid (AP) and tetraploid plants (BP) and between six-month-old seedlings of diploid (AD) and tetraploid plants (BD). A total of 11,547 unigenes overlapped between BPvsAP and BDvsAD. (b) The overlapping unigenes between protocorm-like bodies and seedlings of diploid plants and between protocorm-like bodies and seedlings of tetraploid plants. A total of 1591 unigenes overlapped between ADvsAP and BPvsBD. AP—protocorm-like bodies of diploid plants; BP—protocorm-like bodies of tetraploid plants; AD—six-month-old seedlings of diploid plants; BD—six-month-old seedlings of tetraploid plants.

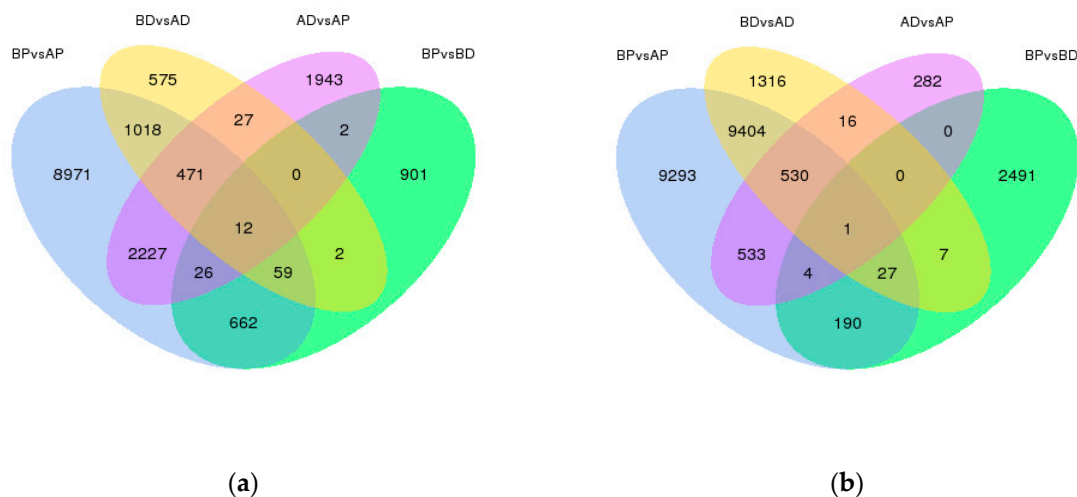


Figure 7. Analysis of differentially expressed genes (DEGs) by comparison between diploid (A) and tetraploid (B) *D. officinale* hybrid plants (201-1 and 201-1-T, respectively) at the stages of protocorm-like bodies (P) and six-month-old seedlings (D). The overlapping portions of the different circles represent the number of DEGs common to these comparison groups: (a) up-regulated differential expression genes; (b) down-regulated differential expression genes. AP—protocorm-like bodies of diploid plants; BP—protocorm-like bodies of tetraploid plants; AD—six-month-old seedlings of diploid plants; BD—six-month-old seedlings of tetraploid plants.

After filtration, 33,428 DEGs between the PLBs of tetraploid (BP) and diploid plants (AP), as well as 13,465 DEGs between the seedlings of tetraploid (BD) and diploid plants (AD), were obtained (Figure 6a). A total of 6074 genes were differentially expressed between AD and AP, and 4384 genes were differentially expressed between BP and BD (Figure 6b). There were 11,547 unigenes that overlapped between BPvsAP and BDvsAD, and 1591 unigenes in common between ADvsAP and BPvsBD.

Within 33,428 DEGs, there were 13,446 up-regulated and 19,982 down-regulated DEGs between PLBs of tetraploid and diploid plants (BPvsAP) (Figure 7). Similarly, within 13,456 DEGs, 2164 up-regulated and 11,301 down-regulated DEGs were identified, respectively, between seedlings of tetraploid and diploid plants (BDvsAD).

Among pairwise comparisons for up-regulation, the highest number of DEGs (8971) was observed for BPvsAP (8971), followed by ADvsAP (1943), BPvsBD (901), and BDvsAD (575) (Figure 6a). Similarly, the highest number of DEGs for down-regulation was detected in BPvsAP (9239), followed by BPvsBD (2491), BDvsAD (1316), and ADvsAP (282) (Figure 6b).

3.4. GO and KEGG of DEGs Annotation and Enrichment Analysis

All DEGs between the genotypes (diploid—A vs. tetraploid—B) and organs (PLBs—P vs. six-month-old seedlings—D) were used to perform GO and KEGG enrichment analyses. The GO annotation statistics were used for the DEGs in pairs. For example, the up-regulation of GO enrichment in the BP vs. AP comparison was mainly observed in two groups of biological processes (BP) (e.g., carbohydrate metabolic process, 513; monocarboxylic acid metabolic process, 230; organic acid biosynthetic process, 225; and carboxylic acid biosynthetic process, 225) and molecular function (MF) (e.g., catalytic activity, 3943; cofactor binding, 287; and coenzyme binding, 242) (Figure 8a). In contrast, the down-regulation of GO enrichment in the BP vs. AP comparison was scattered and correlated in all three groups of BP (e.g., biosynthetic process, 2811; organic substance biosynthetic process, 2717; and cellular biosynthetic process, 2589), cellular component (CC) (e.g., intracellular organelle, 2359; cell and cell part, 3472), and MF (e.g., catalytic activity, 5485; oxidoreductase activity, 1087; and transferase activity, 2187) (Figure 8b). Other pairwise comparisons are shown in Figure S2.

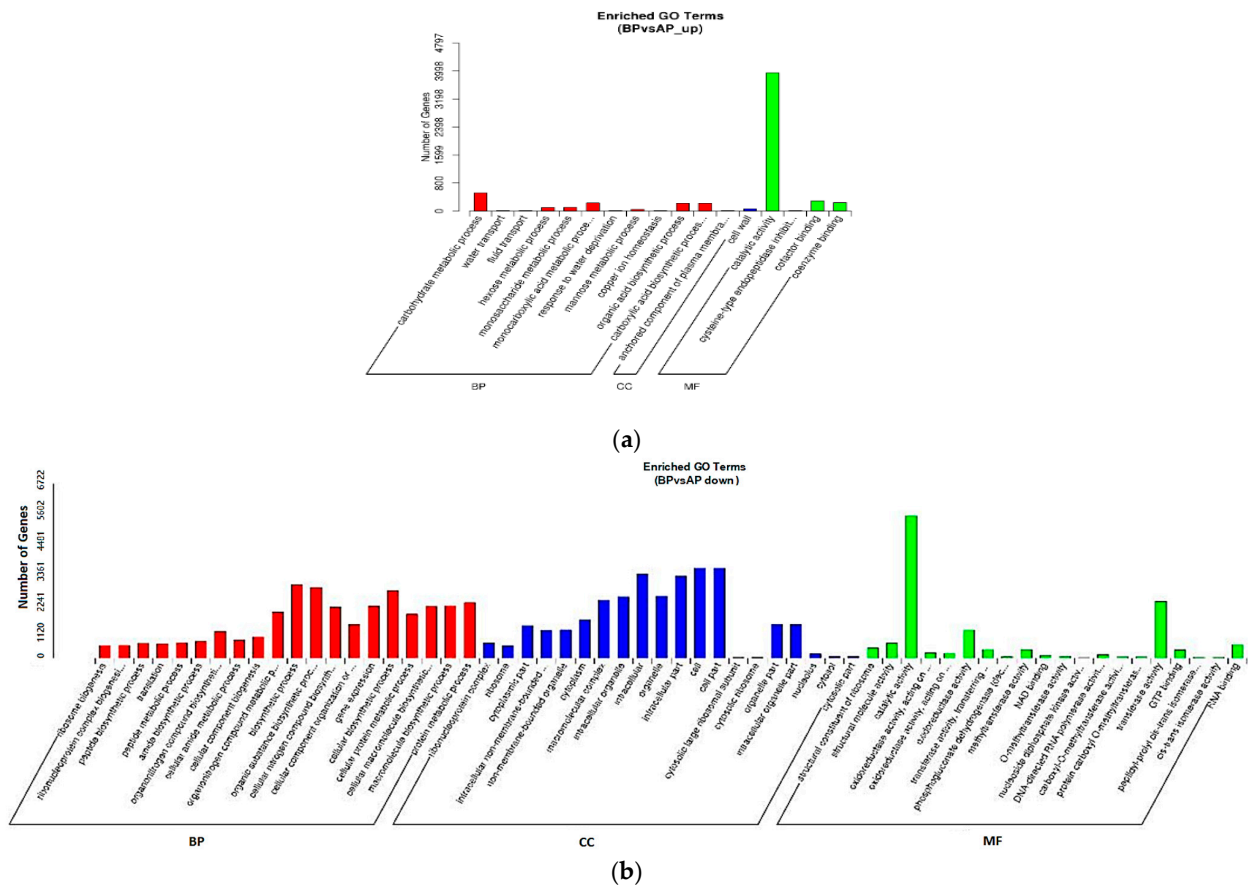


Figure 8. Pairwise GO enrichment analysis of DEGs in protocorm-like bodies of diploid and tetraploid *D. officinale*. The bottom x-axis represents each detailed classification of GO. The upper y-axis indicates the number of DEGs annotated to a GO term: (a) GO enrichment analysis of up-regulated DEGs; (b) GO enrichment analysis of down-regulated DEGs. AP—protocorm-like bodies of diploid plants; BP—protocorm-like bodies of tetraploid plants; BP—biological process; CC—cellular component; MF—molecular function.

For KEGG enrichment of DEGs for the top 20 pathways, the pairwise comparisons of AP vs. BP showed that the pathways “protein processing endoplasmic reticulum”, “Glycolysis/Gluconeogenesis”, and citrate cycle (TCA cycle) were enriched, with 320, 197, and 75 DEGs, respectively (Figure S3a). In the seedlings, the pathway “Protein processing in endoplasmic reticulum” was enriched, with 150 DEGs in the comparison between AD and BD (Figure S3b). Notably, the comparative analysis between BP and BD libraries showed that 46 DEGs were predicted to be involved in “Glyoxylate and dicarboxylate”; and 39 genes in “Glycolysis/Gluconeogenesis”; 35 genes in “Fructose and mannose metabolism”; and 26 DEGs in “pentose phosphate pathway” (Figure S3c). These pathways are related to carbohydrate metabolism. The up-regulated DEGs in the BP vs. AP comparison for the top 20 KEGG pathways were significantly enriched in the spliceosome (121), mRNA surveillance pathway (86), glycolysis/gluconeogenesis (81), viral carcinogenesis (78), ribosome biogenesis in eukaryotes (70), phagosome and herpes simplex infection (57), and galactose metabolism (51) (Figure S4a). The down-regulated DEGs in the BP vs. AP comparison were significantly enriched in ribosome (312), biosynthesis of amino acids (218), protein processing in the endoplasmic reticulum (203), RNA transport (178), ribosome biogenesis in eukaryotes (115), and phagosome (82). Similarly, for the top 20 KEGG pathways, the up-regulated DEGs in the BD vs. AD comparison were significantly correlated in protein processing in the endoplasmic reticulum (31), ubiquitin-mediated proteolysis (23), amino sugar and nucleotide sugar metabolism (22), lysosome (20), phagosome (15), and non-alcoholic fatty liver disease (14) (Figure S4b). The down-regulated DEGs in the BD vs. AD comparison were significantly enriched in ribosome (151), protein processing in the endoplasmic reticulum (119), glycolysis/ gluconeogenesis (77), ribosome biogenesis in eukaryotes (70), phagosome (61), glutathione metabolism (47), drug metabolism-cytochrome P450 (37), and pentose phosphate pathway (36).

3.5. qRT-PCR Validation for Genes Involved in Polysaccharide Biosynthesis between Diploid and Tetraploid *D. officinale*

Since changes in the polysaccharide contents were observed in tetraploid plants [24], and mannose is the major monosaccharide in *D. officinale*, genes related to mannan polysaccharide biosynthesis were of interest and were validated on both diploid and tetraploid *D. officinale* hybrid lines, viz. 201-1, 201-1-T, 201-3, and 201-3-T (Table 1). These genes, which encoded enzymes that catalyze reactions in the biosynthesis of polysaccharides, were identified from DEG databases. In this study, we randomly selected 11 genes to examine gene expression using qRT-PCR, including (1) cellulose synthase-like A (CSLA, EC: 2.4.1.32—*DoCSLA3-1*), which encodes mannan synthase that catalyzes the formation of mannan polysaccharide from GDP-D-mannose or GDP-D-glucose; (2) glucose-1-phosphate adenylyltransferase (glgC, EC: 2.7.7.27—*DoglgC1*, *DoglgC3*), which catalyzes the reaction between ATP and alpha-D-glucose 1-phosphate (G1P) to produce pyrophosphate and ADP-Gl; (3) GDP-mannose pyrophosphorylase (GMPP, EC: 2.7.7.13, mannose-1-phosphate guanylyltransferase—*DoGMPP-1*, *DoGMPP-2*, *DoGMPP-3*), which catalyzes the conversion of mannose-1-phosphate to GDP-mannose; (4) 2,3-bisphosphoglycerate-independent phosphoglycerate mutase (gmpI, EC: 5.4.2.12—*DogmpI*); (5) mannan endo-1,4-beta-mannosidase (MAN, EC: 3.2.1.78—*DoMAN2-2*), which digests manno-polysaccharides’ function in cell wall metabolism; (6) phosphoglucomutase (PGM, EC: 5.4.2.2—*DoPGM1*, *DoPGM2-2*), which catalyzes the interconversion of glucose-1-phosphate and glucose-6-phosphate; and (7) phosphomanomutase (PMM, EC: 5.4.2.8—*DoPMM2-1*), which catalyzes the interconversion of manose-6-phosphate to mannose-1-phosphate (Table S3).

As expected, these genes exhibited consistent expression tendencies. The qRT-PCR data for these genes corroborated the findings from the RNA-Seq data analyses (Figure 9). This implies that the RNA-Seq data are accurate and valuable. Additionally, in most cases, the expression of these in the tetraploid 201-1-T was higher than in the diploid 201-1, except for *DoPGM1-1* and *DoPMM2*.

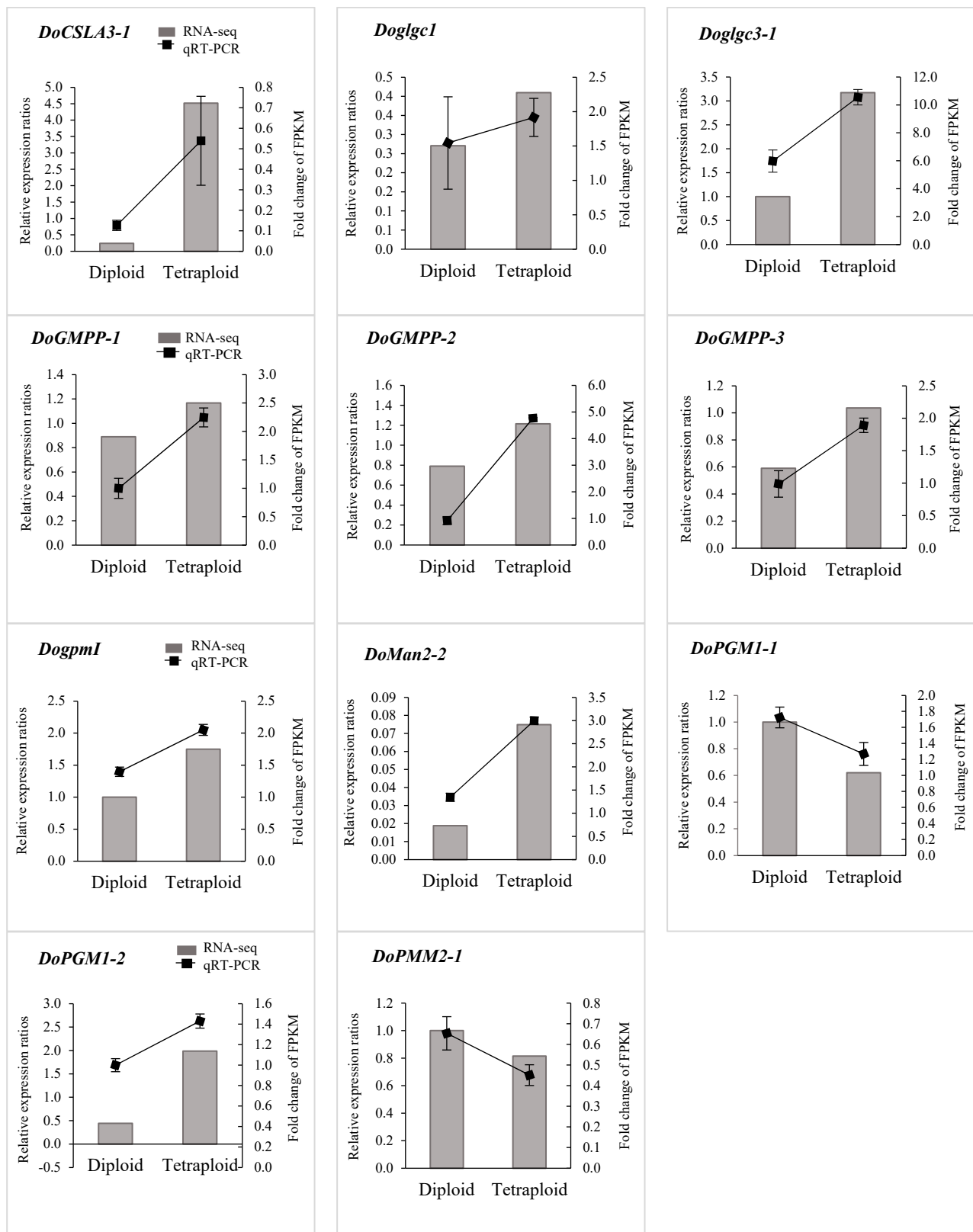


Figure 9. qRT-PCR confirmation of 11 genes expressed in diploid and tetraploid *D. officinale*. The expression patterns of selected genes were analyzed across diploid and tetraploid plants. Gray bars represent the FPKM values according to RNA-Seq (right y-axis). Black lines indicate the relative expression level determined by qRT-PCR (left y-axis), with error bars.

4. Discussion

D. officinale has been an effective traditional Chinese medicine for thousands of years and is customarily used for a wide range of ailments in many Asian countries [55]. Previous studies have reported that bioactive compounds, including phenolic acids and polysaccharides, contribute to the pharmacological properties of *D. officinale*, and the quality of this plant as well. Some previous studies have indicated that polyploidy causes remarkable changes in morphological and physiological traits, which may also enhance the content of secondary metabolites and improve growth rates and genetic quality. Our previous study also revealed tetraploid *D. officinale* that was selected from a regenerated population of “201-1” after the PLBs were treated with colchicine, which contained an especially high polysaccharide content [39]. In addition, the polysaccharide content in the stem was the highest, followed by the leaf and root [39], which may explain why the stems of this species are widely used for medical purposes [55,56]. However, the differentiation in molecular mechanisms controlling the polysaccharide content between diploid and tetraploid *D. officinale* has remained unknown. A few studies have conducted transcriptome analyses for *D. officinale* considering different growth stages (juvenile to adult) [41], different plant parts (leaves, stems and roots) [43], flowers [57], and 2-year-old stems [58], and there have been studies on other *Dendrobium* species, such as *D. huoshanense* [57,59,60], *D. catenatum* [61], and *D. moniliforme* [62]. Therefore, this study has investigated transcriptomic profiles and some key genes related to polysaccharide biosynthesis tetraploid *D. officinale*.

In this study, PLBs and six-month-old seedlings of diploid and tetraploid *D. officinale* 201-1 were used to generate four transcriptomic libraries and examine the critical genes associated with polysaccharides. A total of 235,443,082 raw reads and 230,786,618 clean reads with a total of 34.62 Gb nucleotides were obtained (Table 1). After Trinity de novo assembly and quality control, a total of 274,403 unigenes were obtained, of which 10.58–66.95% were annotated in each of the seven databases (NR, NT, KO, Swiss-Prot, FAM, GO, and KOG) and 6.35% were annotated in all seven databases (Table 3). The unigenes showed significant homology with the top five species, including *P. dactylifera*, *E. guineensis*, *N. nucifera*, *M. acuminata*, and *V. vinifera*, with a homology range of 3.2–27.7%, but 30.4% of the contigs remained unknown (Figure 2c).

GO, KOG, and KEGG classified 89,827, 29,057, and 34,394 unigenes into 57, 25, and 19 functional groups, respectively (Figures 3, 4 and S1). GO classification provided overall insight into their expression and showed the top three GO terms, including metabolic and cellular processes and binding and catalytic activity (Figure 3). In the KOG database, the three top terms were R (general function prediction only), O (post-translational modification, protein turnover, and chaperones), and J (translation, ribosome structure, and biogenesis). Similarly, in the KEGG database, the top term was carbohydrate metabolism pathway, with 3986 unigenes. In GO and KEGG enrichment analysis, pairwise comparisons between diploid and tetraploid plants at the growth stages of protocorm-like bodies and six-month-old seedlings were presented in Figures 7 and 8, as well as Supplementary Figures S2 and S3. Notably, the highest DEGs in both the up-regulated and down-regulated groups were for pairwise genes of diploid and tetraploid plants at the protocorm-like body stage (AP vs. BP), with 8971 and 9293, respectively (Figure 7).

qRT-PCR analysis for 11 randomly selected genes demonstrated consistency with RNA-Seq, although 2 out of 11 genes expressed lower levels in tetraploid than in diploid plants (*DoPGM1-1* and *DoPMM2-1*) (Figure 9). Higher numbers of raw reads (235,443,082) and clean reads (230,786,618), as well as a greater size (36.42 Gb), were generated in this study compared with other studies. For example, Zhang et al. [41] generated 102 and 86 million high-quality reads for *D. officinale* for juvenile and adult plants, respectively. The total number of unigenes assembled was, therefore, also higher: 274,403 compared with the 145,791 unigenes previously reported by Zhang et al. [41]. This could be due to the number of libraries integrated, as four libraries were used. Additionally, a total of 203,043 (73.99%) unigenes provided striking BLAST results. This information far exceeded that previously described by Guo et al. [63] (25,473—69.97%) and Zhang et al. [41]

(67,396—46.23% unigenes), which provided sufficient resources to study this *Dendrobium* species. *D. officinale* has a thick, soluble, polysaccharide-rich stem [27,39]. Pham et al. [39] reported that the polysaccharide contents in the stem, leaf, and root of the tetraploid 201-1-T were higher than those in the diploid 201-1, proving that chromosome doubling enhances the production of polysaccharide in *D. officinale*. Consistently, the polysaccharide content in the stem exhibited the highest level, followed by the leaf, while the lowest was found in the root. This aligns with the results of qRT-PCR, where nine out of eleven genes involved in polysaccharide biosynthesis were significantly up-regulated in diploid compared to tetraploid plants (Figure 9).

Polysaccharides are the major and active medicinal components of *D. officinale* [24]. Polysaccharide biosynthesis involves three key stages: (1) sucrose produced by photosynthesis in the chloroplast is converted into glucose 1-phosphate (Glc-1P) and fructose-6-phosphate via a series of enzymatic reactions, such as HK, PGM, UPG, USP, scrK, FBP-base, etc. [24,27]. (2) These two monosaccharides (glucose 1-phosphate and fructose-6-phosphate) are extended into various nucleotide-diphospho-sugars (NDP sugars) by enzymatic reactions, including PMM, GMPP, GMDS, UXE, UGD, USP, RHM, UGE, etc. (3) All NDP-sugars are transformed into macromolecular polysaccharides through successive catalysis by different kinds of glycosyltransferases (GTs) [64], such as glucosyltransferases, mannosyltransferases, fucosyltransferases, and xylosyltransferases [24,27,41]. In this study, we identified 127, 94, 26, and 29 genes for glucosyltransferases, mannosyltransferases, fucosyltransferases, and xylosyltransferases, respectively (Supplementary Table S2). Zhang et al. [41] also identified 430 possible GTs in the *D. officinale* transcriptome database, which were divided into 35 GT families. Randomly selected genes of *glgC*, *GMPP*, *gpml*, *Man2*, *PGM*, and *PMM* (Table S3) for RT-PCR were involved in the first two stages.

Mannan polysaccharides are known to accumulate in the stems of *D. officinale*. These soluble polysaccharides are synthesized from mannose, glucose, and galactose at a molar ratio of 223:48:1 [40,65]. Their contents account for 58.3% of the dry weight of the crude polysaccharide fraction in *D. officinale* [66]. The biosynthesis of mannan polysaccharides is catalyzed by mannan synthase, which is encoded by members of the cellulose synthase-like A (CSLA) family [40,65]. For example, CSLA genes from *Arabidopsis thaliana* encode mannan synthase, which actively participates in the synthesis of polysaccharides [67]. In our transcriptomic analysis, we also identified genes belonging to the CSLA family and randomly selected a Cluster-29035.190181 (*DoCSLA3-1*). *CSLA3* is one out of the four CSLA genes, i.e., *CSLA2*, *CSLA3*, *AtCSLA7*, and *AtCSLA9*, participating in the production of mannan polysaccharides in *Arabidopsis*. Moreover, *AtCSLA2*, 3, and 9 contribute to the synthesis of glucomannan in the stems. These *CSLA3* showed higher expression in tetraploid *D. officinale* than in this diploid. This is in agreement with the previous study by Goubet et al. [66]: the most abundant transcripts of the *DoCSLA3* gene were found in the stems. Moreover, higher expression levels of GMPP and PGM were positively correlated with higher contents of polysaccharides, consistent with the findings of Wang et al. [27]. Expressions for one gene-encoding PGM (*DoPGM1-1*) and gene-encoding PMM (*DoPMM2-1*), bifunctional enzymes, were decreased in tetraploid plants, and this was negatively correlated with the *D. officinale* polysaccharide content. This might imply that these bifunctional enzymes have a greater capacity for degradation than polysaccharide biosynthesis. Consequently, the characterization of the content of DOPs in tetraploid *D. officinale* using comparative transcriptome sequencing identified putative genes encoding enzymes that participated in the metabolism of DOPs in tetraploid plants.

5. Conclusions

The comparative RNA-Seq analysis of diploid and tetraploid *D. officinale* PLBs and the stems of six-month-old seedlings enabled the identification of candidate genes encoding enzymes involved in polysaccharide biosynthesis. This study also provides insight explaining the increased polysaccharide contents in autopoloidy. To the best of our knowledge, we have presented, for the first time, a comparative transcriptome analysis and polysaccha-

rides of diploid and tetraploid *D. officinale*. Additionally, the genes involved in regulating polysaccharide biosynthesis displayed differential expression in the stems of diploid and tetraploid *D. officinale*, which was consistent with RNA-Seq data.

Supplementary Materials: The following supporting information can be downloaded at: <https://www.mdpi.com/article/10.3390/agronomy14010069/s1>, Figure S1: KEGG classifications of *D. officinale* unigenes; Figure S2: Pairwise comparisons of GO enrichment analysis of DEGs in diploid; Figure S3: Pairwise KEGG enrichment analysis of DEGs of diploid and tetraploid *D. officinale* for the top 20 pathways at growth stages of protocorm-like bodies and six-month-old seedlings; Figure S4: Pairwise KEGG enrichment analysis of DEGs in protocorm-like bodies and six-month-old seedlings of diploid and tetraploid *D. officinale* for the top 20 pathways; Table S1: Growth stages and growth conditions applied for diploid 201-1 (A) and tetraploid 201-1-T (B) *D. officinale* used for transcriptome analysis; Table S2: Polysaccharide, manose; Table S3: Primers used in qRT-PCR for 11 selected genes: GAPDH and Actin genes.

Author Contributions: Conceptualization, P.L.P.; methodology, R.-Z.Z., L.X. and Z.-S.Z.; software, P.L.P., V.T.H.T. and T.T.C.L.; investigation, P.L.P., T.T.H.V. and T.T.N.; resources, P.L.P., V.T.H.T., M.N.N. and Z.-S.Z.; visualization, P.L.P., R.-Z.Z., T.D.X. and T.D.K.; validation, L.X., T.D.X., M.N.N. and P.L.P.; writing—original draft preparation, P.L.P., V.T.H.T., M.N.N. and L.X.; writing—review and editing, T.D.X., T.D.K. and T.T.N.; supervision, R.-Z.Z. and Z.-S.Z. All authors have read and agreed to the published version of the manuscript.

Funding: This research was partially funded by Vietnam National University of Agriculture for project “Research on generating polyploid lines of *Dendrobium officinale* to increase polysaccharide content for medicinal processing” (No. T2021-01-01TD).

Institutional Review Board Statement: Not applicable.

Data Availability Statement: The data presented in this study are available upon request from the corresponding author. The data are not publicly available due to privacy concerns.

Acknowledgments: The authors would like to sincerely thank to the Board of Directors and colleagues of Vietnam National University of Agriculture for their support to complete this work. The great thanks also send to my supervisors at College of Forestry and landscape Architecture, South China Agricultural University, Guangzhou, China for genetic data analyses, National Engineering Research Center of Plant Space Breeding, China for providing the experimental conditions, and special thanks to Jun-Min Liu for her help on determination of polysaccharides contents. We also thank the grateful collaboration between South China Agricultural University and Vietnam National University of Agriculture. The authors highly appreciated four anonymous reviewers for their valuable comments and suggestions to improve the quality of this work.

Conflicts of Interest: The authors declare no conflicts of interest.

References

1. Mohammed, A.S.A.; Naveed, M.; Jost, N. Polysaccharides; classification, chemical properties, and future perspective applications in fields of pharmacology and biological medicine (A review of current applications and upcoming potentialities). *J. Polym. Environ.* **2021**, *29*, 2359–2371. [[CrossRef](#)] [[PubMed](#)]
2. Claus-Desbonnet, H.; Nikly, E.; Nalbantova, V.; Karcheva-Bahchevanska, D.; Ivanova, S.; Pierre, G.; Benbassat, N.; Katsarov, P.; Michaud, P.; Lukova, P.; et al. Polysaccharides and their derivatives as potential antiviral molecules. *Viruses* **2022**, *14*, 426. [[CrossRef](#)] [[PubMed](#)]
3. Tzianabos, A.O. Polysaccharide immunomodulators as therapeutic agents: Structural aspects and biological function. *Clin. Microbiol. Rev.* **2000**, *13*, 523–533. [[CrossRef](#)] [[PubMed](#)]
4. Cai, W.; Xie, L.; Chen, Y.; Zhang, H. Purification, characterization, and anticoagulant activity of the polysaccharides from green tea. *Carbohydr. Polym.* **2013**, *92*, 1086–1090. [[CrossRef](#)] [[PubMed](#)]
5. Lee, J.S.; Synytsya, A.; Kim, H.B.; Choi, D.J.; Lee, S.; Lee, J.; Kim, W.J.; Jang, S.J.; Park, Y.I. Purification, characterization and immunomodulating activity of a pectic polysaccharide isolated from Korean mulberry fruit Oddi (*Morus alba* L.). *Int. Immunopharmacol.* **2013**, *17*, 858–866. [[CrossRef](#)] [[PubMed](#)]
6. Simpson, R.; Morris, G.A. The anti-diabetic potential of polysaccharides extracted from members of the cucurbit family: A review. *Bioact. Carbohydr. Diet. Fibre* **2014**, *3*, 106–114. [[CrossRef](#)]
7. Xie, S.Z.; Liu, B.; Zhang, D.D.; Zha, X.Q.; Luo, J.P. Intestinal immunomodulating activity and structural characterization of a new polysaccharide from stems of *Dendrobium officinale*. *Food Funct.* **2016**, *7*, 2789–2799. [[CrossRef](#)]

8. Chen, W.H.; Wu, J.J.; Li, X.F.; Lu, J.M.; Wu, W.; Sun, Y.Q.; Zhu, B. Isolation, structural properties, bioactivities of polysaccharides from *Dendrobium officinale* Kimura et. Migo: A review. *Int. J. Biol. Macromol.* **2021**, *184*, 1000–1013. [[CrossRef](#)]
9. Zhu, S.; Niu, Z.; Xue, Q.; Wang, H.; Xie, X.; Ding, X. Accurate authentication of *Dendrobium officinale* and its closely related species by comparative analysis of complete plastomes. *Acta Pharm. Sin. B* **2018**, *8*, 969–980. [[CrossRef](#)]
10. Xu, J.; Han, Q.B.; Li, S.L.; Chen, X.J.; Wang, X.N.; Zhao, Z.Z.; Chen, H.B. Chemistry, bioactivity and quality control of *Dendrobium*, a commonly used tonic herb in traditional Chinese medicine. *Phytochem. Rev.* **2013**, *12*, 341–367. [[CrossRef](#)]
11. Niu, Z.; Zhu, F.; Fan, Y.; Li, C.; Zhang, B.; Zhu, S.; Hou, Z.; Wang, M.; Yang, J.; Xue, Q.; et al. The chromosome-level reference genome assembly for *Dendrobium officinale* and its utility of functional genomics research and molecular breeding study. *Acta Pharm. Sin. B* **2021**, *11*, 2080–2092. [[CrossRef](#)] [[PubMed](#)]
12. Kamemoto, H.; Amore, T.D.; Kuehnle, A.R. *Breeding Dendrobium Orchids in Hawaii*; University of Hawaii Press: Honolulu, HI, USA, 1999; 176p.
13. Zhang, X.; Gao, J. In vitro tetraploid induction from multigenotype protocorms and tetraploid regeneration in *Dendrobium officinale*. *Plant Cell Tissue Organ Cult.* **2020**, *141*, 289–298. [[CrossRef](#)]
14. Teixeira da Silva, J.A.; Zeng, S.; Galdiano, R.F., Jr.; Dobrańszki, J.; Cardoso, J.C.; Vendrame, W.A. In vitro conservation of *Dendrobium* germplasm. *Plant Cell Rep.* **2014**, *33*, 1413–1423. [[CrossRef](#)] [[PubMed](#)]
15. Hossain, M.M.; Kant, R.; Van, P.T.; Winarto, B.; Zeng, S.; Teixeira da Silva, J.A. The application of biotechnology to orchids. *Crit. Rev. Plant Sci.* **2013**, *32*, 69–139. [[CrossRef](#)]
16. Manzoor, A.; Ahmad, T.; Bashir, M.A.; Hafiz, I.A.; Silvestri, C. Studies on colchicine induced chromosome doubling for enhancement of quality traits in ornamental plants. *Plants* **2019**, *8*, 194. [[CrossRef](#)]
17. Atichart, P. Polyploid induction by colchicine treatments and plant regeneration of *Dendrobium chrysotoxum*. *Thai J. Agric. Sci.* **2013**, *46*, 59–63.
18. Li, H.; Zheng, X.S.; Long, C.L. Induction of polyploid of *Dendrobium devonianum*. *Acta Bot. Yunnanica* **2005**, *27*, 552–556. (In Chinese with English abstract)
19. Vichiato, M.R.M.; Vichiato, M.; Pasqual, M.; Rodrigues, F.A.; Castro, D.M. Morphological effects of induced polyploidy in *Dendrobium nobile* Lindl. (Orchidaceae). *Crop Breed. Appl. Biotechnol.* **2014**, *14*, 154–159. [[CrossRef](#)]
20. Wang, A.H.; Wu, Q.Q.; Yang, L.; Xu, H.J.; Chen, Z.L. Study on polyploid of *Dendrobium ochreatum* induced by colchicine. *J. Southwest Univ.* **2017**, *39*, 55–60. (In Chinese with English abstract)
21. Zhan, Z.G.; Cheng, X.U. Study on colchiploid of *Dendrobium officinale* induced by colchicines. *J. Zhejiang Univ.* **2011**, *38*, 321–325. (In Chinese with English abstract)
22. Liu, Y.; Duan, S.-D.; Jia, Y.; Hao, L.-H.; Xiang, D.-Y.; Chen, D.-F.; Niu, S.-C. Polyploid Induction and Karyotype Analysis of *Dendrobium officinale*. *Horticulturae* **2023**, *9*, 329. [[CrossRef](#)]
23. Bulpitt, C.J.; Li, Y.; Bulpitt, P.F.; Wang, J. The use of orchids in Chinese medicine. *J. R. Soc. Med.* **2007**, *100*, 558–563. [[CrossRef](#)] [[PubMed](#)]
24. Yan, L.; Wang, X.; Liu, H.; Tian, Y.; Lian, J.M.; Yang, R.; Hao, S.; Wang, X.; Yang, S.; Li, Q.; et al. The genome of *Dendrobium officinale* illuminates the biology of the important traditional Chinese orchid herb. *Mol. Plant* **2015**, *8*, 922–934. [[CrossRef](#)] [[PubMed](#)]
25. Tang, H.X.; Zhao, T.W.; Sheng, Y.J.; Zheng, T.; Fu, L.Z.; Zhang, Y.S. *Dendrobium officinale* Kimura et Migo: A review on its ethnopharmacology, phytochemistry, pharmacology, and industrialization. *Evid. Based Complement. Altern. Med.* **2017**, *2017*, 7436259. [[CrossRef](#)] [[PubMed](#)]
26. Mai, Y.; Yang, Z.; Ji, X.; An, W.; Huang, Y.; Liu, S.; He, L.; Lai, X.; Huang, S.; Zheng, X. Comparative analysis of transcriptome and metabolome uncovers the metabolic differences between *Dendrobium officinale* protocorms and mature stems. *All Life* **2020**, *13*, 346–359. [[CrossRef](#)]
27. Wang, Z.; Jiang, W.; Liu, Y.; Meng, X.; Su, X.; Cao, M.; Wu, L.; Yu, N.; Xing, S.; Peng, D. Putative genes in alkaloid biosynthesis identified in *Dendrobium officinale* by correlating the contents of major bioactive metabolites with genes expression between protocorm-like bodies and leaves. *BMC Genom.* **2021**, *22*, 579. [[CrossRef](#)] [[PubMed](#)]
28. Zhang, P.; Zhang, X.; Zhu, X.; Hua, Y. Chemical constituents, bioactivities, and pharmacological mechanisms of *Dendrobium officinale*: A review of the past decade. *J. Agric. Food Chem.* **2023**, *71*, 14870–14889. [[CrossRef](#)] [[PubMed](#)]
29. Zhang, M.; Yu, Z.; Zeng, D.; Si, C.; Zhao, C.; Wang, H.; Li, C.; He, C.; Duan, J. Transcriptome and metabolome reveal salt-stress responses of leaf tissues from *Dendrobium officinale*. *Biomolecules* **2021**, *11*, 736. [[CrossRef](#)]
30. Xing, X.H.; Cui, S.W.; Nie, S.P.; Phillips, G.O.; Goff, H.D.; Wang, Q. Study on *Dendrobium officinale* O-acetyl-glucomannan (Dendronan R): Part II. Fine structures of O-acetylated residues. *Carbohydr. Polym.* **2015**, *117*, 422–433. [[CrossRef](#)]
31. Madani, H.; Eschrich, A.; Hosseini, B.; Sanchez-Muñoz, R.; Khojasteh, A.; Palazon, J. Effect of polyploidy induction on natural metabolite production in medicinal plants. *Biomolecules* **2021**, *11*, 899. [[CrossRef](#)]
32. Yadav, A.K.; Singh, S.; Yadav, S.; Dhyani, D.; Bhardwaj, G.; Sharma, A.; Singh, B. Induction and morpho-chemical characterization of *Stevia rebaudiana* colchiploids. *Indian J. Agric. Sci.* **2013**, *83*, 159–165.
33. Wallaart, T.; Pras, N.; Quax, W.J. Seasonal variations of artemisinin and its biosynthetic precursors in tetraploid *Artemisia annua* plants compared with the diploid wild-type. *Planta Med.* **1999**, *65*, 723–728. [[CrossRef](#)] [[PubMed](#)]
34. Lin, X.; Zhou, Y.; Zhang, J.; Lu, X.; Zhang, F.; Shen, Q.; Wu, S.; Chen, Y.; Wang, T.; Tang, K. Enhancement of artemisinin content in tetraploid *Artemisia annua* plants by modulating the expression of genes in artemisinin biosynthetic pathway. *Biotechnol. Appl. Biochem.* **2011**, *58*, 50–57. [[CrossRef](#)] [[PubMed](#)]

35. Gao, S.L.; Zhu, D.N.; Cai, Z.H.; Xu, D.R. Autotetraploid plants from colchicine treated bud culture of *Salvia miltiorrhiza* Bge. *Plant Cell Tissue Organ Cult.* **1996**, *47*, 73–77. [[CrossRef](#)]
36. Gao, S.L.; Chen, B.J.; Zhu, D.N. In vitro production and identification of autotetraploids of *Scutellaria baicalensis*. *Plant Cell Tissue Organ Cult.* **2002**, *70*, 289–293. [[CrossRef](#)]
37. Kim, Y.S.; Hahn, E.J.; Murthy, H.N.; Paek, K.Y. Effect of polyploidy induction on biomass and ginsenoside accumulations in adventitious roots of ginseng. *J. Plant Biol.* **2004**, *47*, 356–360. [[CrossRef](#)]
38. Lavania, U.C.; Srivastava, S.; Lavania, S.; Basu, S.; Misra, N.K.; Mukai, Y. Autopolyploidy differentially influences body size in plants, but facilitates enhanced accumulation of secondary metabolites, causing increased cytosine methylation. *Plant J.* **2012**, *71*, 539–549. [[CrossRef](#)] [[PubMed](#)]
39. Pham, P.L.; Li, Y.X.; Guo, H.R.; Zeng, R.Z.; Xie, L.; Zhang, Z.S. Changes in morphological characteristics, regeneration ability, and polysaccharide content in tetraploid *Dendrobium officinale*. *Hortscience* **2019**, *54*, 1879–1886. [[CrossRef](#)]
40. He, C.; Zhang, J.; Liu, X.; Zeng, S.; Wu, K.; Yu, Z.; Wang, X.; Teixeira da Silva, J.A.; Lin, Z.; Duan, J. Identification of genes involved in biosynthesis of mannan polysaccharides in *Dendrobium officinale* by RNA-seq analysis. *Plant Mol. Biol.* **2015**, *88*, 219–231. [[CrossRef](#)]
41. Zhang, J.; He, C.; Wu, K.; Teixeira da Silva, J.A.; Zeng, S.; Zhang, X.; Yu, Z.; Xia, H.; Duan, J. Transcriptome analysis of *Dendrobium officinale* and its application to the identification of genes associated with polysaccharide synthesis. *Front. Plant Sci.* **2016**, *7*, 5. [[CrossRef](#)]
42. Shen, C.; Guo, H.; Chen, H.; Shi, Y.; Meng, Y.; Lu, J.; Feng, S.; Wang, H. Identification and analysis of genes associated with the synthesis of bioactive constituents in *Dendrobium officinale* using RNA-Seq. *Sci. Rep.* **2017**, *7*, 187. [[CrossRef](#)] [[PubMed](#)]
43. Yuan, Y.; Zhang, B.; Tang, X.; Zhang, J.; Lin, J. Comparative transcriptome analysis of different *Dendrobium* species reveals active ingredients-related genes and pathways. *Int. J. Mol. Sci.* **2020**, *21*, 861. [[CrossRef](#)] [[PubMed](#)]
44. Grabherr, M.; Haas, B.; Yassour, M.; Levin, J.Z.; Thompson, A.A.; Amit, I.; Adiconis, X.; Fan, L.; Raychowdhury, R.; Zeng, Q.; et al. Full-length transcriptome assembly from RNA-Seq data without a reference genome. *Nat. Biotechnol.* **2011**, *29*, 644–652. [[CrossRef](#)] [[PubMed](#)]
45. Pruitt, K.D.; Tatusova, T.; Brown, G.R.; Maglott, D.R. NCBI Reference Sequences (RefSeq): Current status, new features, and genome annotation policy. *Nucleic Acids Res.* **2012**, *40*, D130–D135. [[CrossRef](#)] [[PubMed](#)]
46. Ashburner, M.; Ball, C.A.; Blake, J.A.; Botstein, D.; Butler, H.; Cherry, J.M.; Davis, A.P.; Dolinski, K.; Dwight, S.S.; Eppig, J.T.; et al. Gene ontology: Tool for the unification of biology. *Nat. Genet.* **2000**, *25*, 25–29. [[CrossRef](#)] [[PubMed](#)]
47. Kanehisa, M.; Goto, S. KEGG: Kyoto encyclopaedia of genes and genomes. *Nucleic Acids Res.* **2000**, *28*, 27–30. [[CrossRef](#)]
48. Boeckmann, B.; Bairoch, A.; Apweiler, R.; Bökör, M.C.; Estreicher, A.; Gasteiger, E.; Martin, M.J.; Midchoud, K.; O'Donovan, C.; Phan, I.; et al. The Swiss-prot protein knowledgebase and its supplement trembl in 2003. *Nucleic Acids Res.* **2003**, *31*, 365–370. [[CrossRef](#)]
49. Finn, R.D.; Coghill, P.; Eberhardt, R.Y.; Eddy, S.R.; Mistry, J.; Mitchell, A.L.; Potter, S.C.; Punta, M.; Qureshi, M.; Sangrador-Vegas, A.; et al. The Pfam protein families database: Towards a more sustainable future. *Nucleic Acids Res.* **2016**, *44*, D279–D285. [[CrossRef](#)]
50. Szklarczyk, D.; Franceschini, A.; Wyder, S.; Forslund, K.; Heller, D.; Huerta-Cepas, J.; Simonovic, M.; Roth, A.; Santos, A.; Tsafou, K.P.; et al. STRING v10: Protein–protein interaction networks, integrated over the tree of life. *Nucleic Acids Res.* **2015**, *43*, D447–D452. [[CrossRef](#)]
51. Götz, S.; García-Gómez, J.M.; Terol, J.; Williams, T.D.; Nagaraj, S.H.; Nueda, M.J.; Robles, M.; Talón, M.; Dopazo, J.; Conesa, A. High-throughput functional annotation and data mining with the Blast2GO suite. *Nucleic Acids Res.* **2008**, *36*, 3420–3435. [[CrossRef](#)]
52. Li, B.; Dewey, C.N. RSEM: Accurate transcript quantification from RNA-seq data with or without a reference genome. *BMC Bioinform.* **2011**, *12*, 323. [[CrossRef](#)] [[PubMed](#)]
53. Robinson, M.D.; McCarthy, D.J.; Smyth, G.K. edgeR: A Bioconductor package for differential expression analysis of digital gene expression data. *Bioinformatics* **2010**, *26*, 139–140. [[CrossRef](#)] [[PubMed](#)]
54. Livak, K.J.; Schmittgen, T.D. Analysis of relative gene expression data using real-time quantitative PCR and the $2^{-\Delta\Delta C_t}$ method. *Methods* **2001**, *25*, 402–408. [[CrossRef](#)]
55. Wang, Y.; Tong, Y.; Adjobi, O.I.; Wang, Y.; Liu, A. Research advances in multi-omics on the traditional Chinese herb *Dendrobium officinale*. *Front. Plant Sci.* **2022**, *12*, 808228. [[CrossRef](#)] [[PubMed](#)]
56. Zhou, P.; Pu, T.; Gui, C.; Zhang, X.; Gong, L. Transcriptome analysis reveals biosynthesis of important bioactive constituents and mechanism of stem formation of *Dendrobium huoshanense*. *Sci. Rep.* **2020**, *10*, 2857. [[CrossRef](#)] [[PubMed](#)]
57. Shu, W.; Shi, M.; Zhang, Q.; Xie, W.; Chu, L.; Qiu, M.; Li, L.; Zeng, Z.; Han, L.; Sun, Z. Transcriptomic and metabolomic analyses reveal differences in flavonoid pathway gene expression profiles between two *Dendrobium* varieties during vernalization. *Int. J. Mol. Sci.* **2023**, *24*, 11039. [[CrossRef](#)] [[PubMed](#)]
58. Xu, M.; Liu, X.; Wang, J.; Teng, S.Y.; Shi, J.Q.; Li, Y.Y.; Huang, M.R. Transcriptome sequencing and development of novel genic SSR markers for *Dendrobium officinale*. *Mol. Breed* **2017**, *37*, 18. [[CrossRef](#)]
59. Han, R.; Xie, D.; Tong, X.; Zhang, W.; Liu, G.; Peng, D.; Yu, N. Transcriptomic landscape of *Dendrobium huoshanense* and its genes related to polysaccharide biosynthesis. *Acta Soc. Bot. Pol.* **2018**, *87*, 3574. [[CrossRef](#)]

60. Yuan, Y.; Yu, M.; Jia, Z.; Song, X.; Liang, Y.; Zhang, J. Analysis of *Dendrobium huoshanense* transcriptome unveils putative genes associated with active ingredients synthesis. *BMC Genom.* **2018**, *19*, 978. [[CrossRef](#)]
61. Lei, Z.; Zhou, C.; Ji, X.; Wei, G.; Huang, Y.; Yu, W.; Luo, Y.; Qiu, Y. Transcriptome analysis reveals genes involved in flavonoid biosynthesis and accumulation in *Dendrobium catenatum* from different locations. *Sci. Rep.* **2018**, *8*, 6373–6388. [[CrossRef](#)]
62. Yuan, Y.D.; Zhang, J.C.; Kallman, J.; Liu, X.; Meng, M.J.; Lin, J. Polysaccharide biosynthetic pathway profiling and putative gene mining of *Dendrobium moniliforme* using RNA-Seq in different tissues. *BMC Plant Biol.* **2019**, *19*, 521. [[CrossRef](#)] [[PubMed](#)]
63. Guo, X.; Li, Y.; Li, C.; Luo, H.; Wang, L.; Qian, J.; Luo, X.; Xiang, L.; Song, J.; Sun, C.; et al. Analysis of the *Dendrobium officinale* transcriptome reveals putative alkaloid biosynthetic genes and genetic markers. *Gene* **2013**, *527*, 131–138. [[CrossRef](#)] [[PubMed](#)]
64. Breton, C.; Šnajdrová, L.; Jeanneau, C.; Koča, J.; Imberty, A. Structures and mechanisms of glycosyltransferases. *Glycobiology* **2006**, *16*, 29R–37R. [[CrossRef](#)] [[PubMed](#)]
65. He, C.; Wu, K.; Zhang, J.; Liu, X.; Zeng, S.; Yu, Z.; Zhan, X.; da Silva, J.A.T.; Deng, R.; Tan, J.; et al. Cytochemical localization of polysaccharides in *Dendrobium officinale* and the involvement of *DoCSLA6* in the synthesis of mannan polysaccharides. *Front. Plant Sci.* **2017**, *8*, 1599. [[CrossRef](#)]
66. Xing, X.; Cui, S.W.; Nie, S.; Phillips, G.O.; Goff, H.D.; Wang, Q. Study on *Dendrobium officinale* O-acetyl-glucomannan (Dendronan R): Part I. Extraction, purification, and partial structural characterization. *Bioact. Carbohydr. Diet. Fibre* **2014**, *4*, 74–83. [[CrossRef](#)]
67. Goubet, F.; Barton, C.J.; Mortimer, J.C.; Yu, X.; Zhang, Z.; Miles, G.P.; Richens, J.; Liepman, A.H.; Sefen, K.; Dupree, P. Cell wall glucomannan in *Arabidopsis* is synthesized by CSLA glycosyltransferases and influences the progression of embryogenesis. *Plant J.* **2009**, *60*, 527–538. [[CrossRef](#)]

Disclaimer/Publisher’s Note: The statements, opinions and data contained in all publications are solely those of the individual author(s) and contributor(s) and not of MDPI and/or the editor(s). MDPI and/or the editor(s) disclaim responsibility for any injury to people or property resulting from any ideas, methods, instructions or products referred to in the content.